

# MICROMECHANICAL THERMO-FLUIDIC SINGLE-AXIS YAW RATE SENSOR

Gianluca Piazza and Philip Stephanou

University of California Berkeley

Telephone: 510-642-8713 E-mail: piazza@eecs.berkeley.edu, stephp@newton.berkeley.edu

## ABSTRACT

This paper reports on the design and analysis of a novel thermal single-axis microelectromechanical gyroscope. The gyroscope consists of a heated, pressure driven liquid flowing in a microchannel and two temperature sensors that detect the temperature difference between the two opposite walls of the channel. When an external rotation is applied, the resulting Coriolis acceleration acting on the fluid induces a transverse temperature gradient that is measured by the temperature sensors. Parametric optimization of the gyroscope performance is investigated using numerical methods. Expected sensor response is derived showing good linearity and a rate resolution of  $\sim 0.75$  deg/s.

## INTRODUCTION

Increasing demand for low-cost angular rate sensors for inertial navigation purposes, picture stabilization for digital video cameras, as well as numerous automotive, robotics and military applications has drawn attention to micromachined gyroscopes lately. Several vibrating MEM gyroscopes have been successfully fabricated. These gyroscopes make use of Coriolis acceleration, whereby mass with relative translational velocity experiences lateral forces in proportion to an applied external rate of rotation about an axis normal to its motion. Several micromachined vibrating gyroscopes have been demonstrated, including vibrating shells [1], tuning-forks [2], and vibrating beams [3]. Electrostatic [1], piezoelectric [4], magnetic [5] and piezoresistive [4] transduction mechanisms are most commonly adopted.

This paper reports on the preliminary design and analysis of a novel micromachined yaw rate sensor that measures temperature gradients across the width of a channel induced by the Coriolis acceleration acting on a hot fluid flowing in the microchannel. This design combines the recent advances in micromechanical thermal accelerometer [6] with Coriolis mass flow rate sensors [7] to realize a low-cost, high performance, thermo-fluidic angular rate sensor. Thermal accelerometers are based on buoyancy forces that act on a tiny air bubble in an enclosed chamber [8]. They do not require a solid proof mass and they are compact and sensitive to small accelerations. Coriolis mass flow-rate sensors

derive information about fluid density and flow rate by measuring Coriolis forces acting on a moving fluid inside a vibrating channel. The principle of operation of our gyroscope combines these two physical phenomena to measure angular rate.

A thermo-fluidic analysis of the micromechanical single-axis yaw rate sensor is presented in this paper. A thorough numerical model is derived to describe the performance of the thermo-fluidic gyroscope. The sensitivity of the proposed design to variations of geometrical and thermo-mechanical properties is investigated. Linearity, rate resolution, and sensitivity response of the micromachined gyro are discussed.

## GYROSCOPE OPERATION AND DESIGN

The yaw rate sensor under consideration is based on the interaction of inertial and thermal properties in a laminar, internal pipe flow. The forward and return paths of the fluid, as well as the temperature sensors are represented schematically in Figure 1.

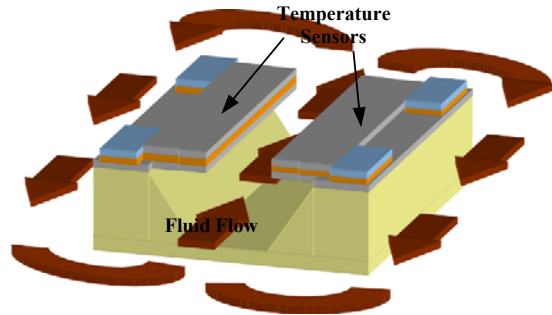


**Fig. 1:** Fluid path and sensor placement for the thermo-fluidic gyroscope

In-plane rotation, or yaw,  $\omega$  of the device induces Coriolis acceleration  $a_c$  normal to the direction of flow of magnitude

$$a_c = 2\omega \times v_x \quad (1)$$

where  $v_x$  is the axial component of the fluid's velocity. The Coriolis acceleration perturbs the parabolic velocity profile of the flow. By assuming that the velocity and pressure gradient,  $\frac{\partial P}{\partial x}$ , are

invariant along the length of the channel, the Navier-Stokes' relations describing the flow can be simplified to a system of nonlinear, coupled ordinary differential equations [9]:

$$\begin{aligned} \rho v_y \frac{\partial v_x}{\partial y} &= \mu \frac{\partial^2 v_x}{\partial y^2} - \frac{\partial P}{\partial x} \\ \rho v_y \frac{\partial v_x}{\partial y} &= \mu \frac{\partial^2 v_y}{\partial y^2} - 2\rho\omega v_x \end{aligned} \quad (2)$$

where  $\rho$ ,  $\mu$ , and  $v_y$  refer to the fluid density, dynamic viscosity and transverse velocity, respectively. The fluid enters the channel at a higher temperature than the surrounding silicon, so the flow loses heat by convection through the channel walls. The resulting temperature profile is given in terms of the above calculated axial and transverse velocity profiles by :

$$v_x \frac{\partial T}{\partial x} + v_y \frac{\partial T}{\partial y} - \alpha \frac{\partial^2 T}{\partial y^2} = 0 \quad (3)$$

where  $\frac{\partial T}{\partial x}$  is constant assuming a uniform rate of heat flux over the length of the channel, and  $\alpha$  is the thermal diffusivity of the fluid. Such a condition could be realized by an equal flow-rate cross-flow heat exchanger [10]. The effect of the Coriolis acceleration on the velocity and temperature profiles is illustrated in Figure 2.

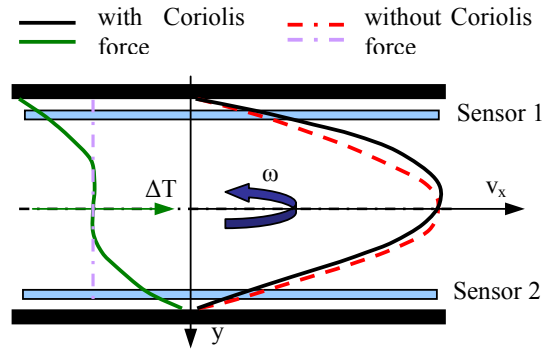


**Fig. 2:** Unperturbed and perturbed velocity and temperature profiles

Solving (2) and (3) yields the yaw-rate as a function of the transverse temperature difference measured by the sensors on opposite walls of the channel. It is assumed that the transverse temperature gradient of (3) does not affect the calculation of the velocity profile in (2).

## GYROSCOPE FABRICATION

The device fabrication process is schematically shown in Figure 3 and it is based on the same technology used for thermal accelerometers [6]. A 0.5  $\mu\text{m}$  thick polysilicon layer is deposited on 0.5  $\mu\text{m}$  thermal oxide. The poly-layer is lightly p-doped to provide low-resistivity sensor elements and optimal ohmic contacts for the bonding pads.

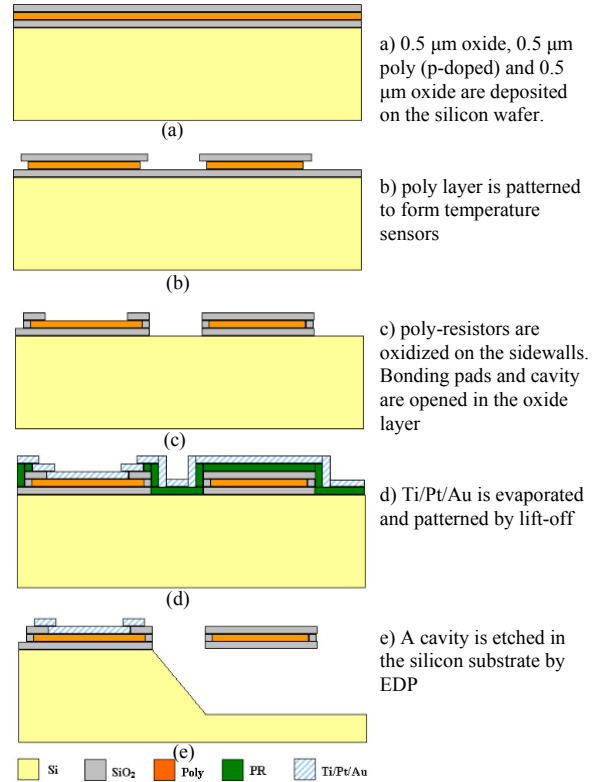


**Fig. 3:** Gyroscope fabrication process flow

An oxidation step is performed to form an oxide-poly-oxide sandwich. Each of the three layers is 0.5  $\mu\text{m}$  thick. The top oxide layer is etched and used as a mask for defining the polysilicon resistive sensors. A short oxidation step is necessary to protect the polysilicon sidewall during ethylene diamine-pyrocatechol (EDP) etch in a later processing step. Bonding pads and cavity windows are opened on the oxide layer and a layer of Ti/Pt/Au is evaporated and patterned by lift-off. Finally the cavity is opened by silicon wet-etch in EDP to form the microchannel. The device is sealed in a hermetic enclosure.

In order to characterize the components constituting the thermo-fluidic gyroscope, specific test structures are designed. The determination of the thermal coefficient of polysilicon is of

fundamental importance in deriving the sensitivity and resolution of the inertial sensor; therefore several size temperature sensors will be fabricated and tested separately. The same resistors will be used to characterize the residual stress in the three layers sandwich. Different length channels will be fabricated to test the change in the gyro response. To verify the intrusiveness of the thermal sensor in the fluid flow, the length and width of the poly-resistors will be appropriately varied and the effects on the gyroscope response recorded.

### EXPECTED TEST RESULTS

The expected results are obtained numerically using MATLAB. The physical properties of the fluid (in this case water) and device specifications that are used in the analysis are summarized in Table 1 and Table 2, respectively.

Thermal diffusivity	Dynamic viscosity	Density
$1.46 \times 10^{-7} \text{ m}^2/\text{s}$	$8.57 \times 10^{-4} \text{ N}\cdot\text{s}/\text{m}^2$	$997 \text{ kg}/\text{m}^3$

**Table 1:** Physical properties of water at 300K

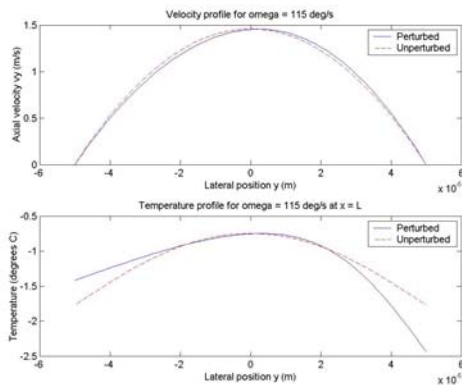
Channel length	Channel width	Pressure drop	Temperature drop
$1 \times 10^{-2} \text{ m}$	$1 \times 10^{-4} \text{ m}$	$-1 \times 10^4 \text{ Pa}$	$-1 \text{ K}$

**Table 2:** Device specifications

Unless otherwise noted, all parameters used to obtain the results below have the values indicated in Table 1 and Table 2.

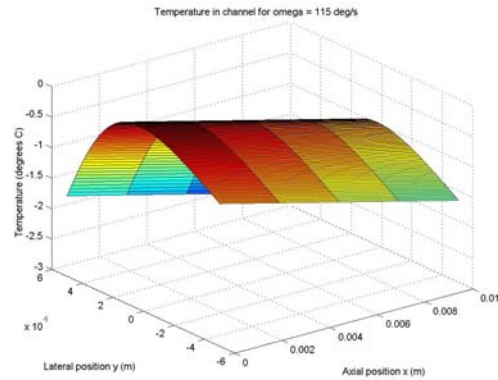
### Fluid Velocity and Temperature Profiles

The unperturbed and perturbed velocity and temperature profiles plotted in Figure 4 are generated by numerically evaluating (2).



**Fig. 4:** Numerically determined unperturbed and perturbed velocity and temperature profiles

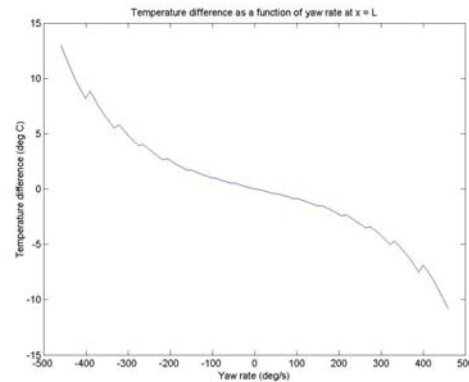
The temperature distribution of the water in the channel assuming a uniform rate of heat flux through the walls is illustrated in Figure 5. The same temperature difference is recorded for each transversal section of the channel. Prescribing uniform wall temperature might be more consistent with the actual physical behavior of the system, but renders the analysis prohibitively complex because of the varying temperature gradient in the axial direction.



**Fig. 5:** Temperature distribution in channel

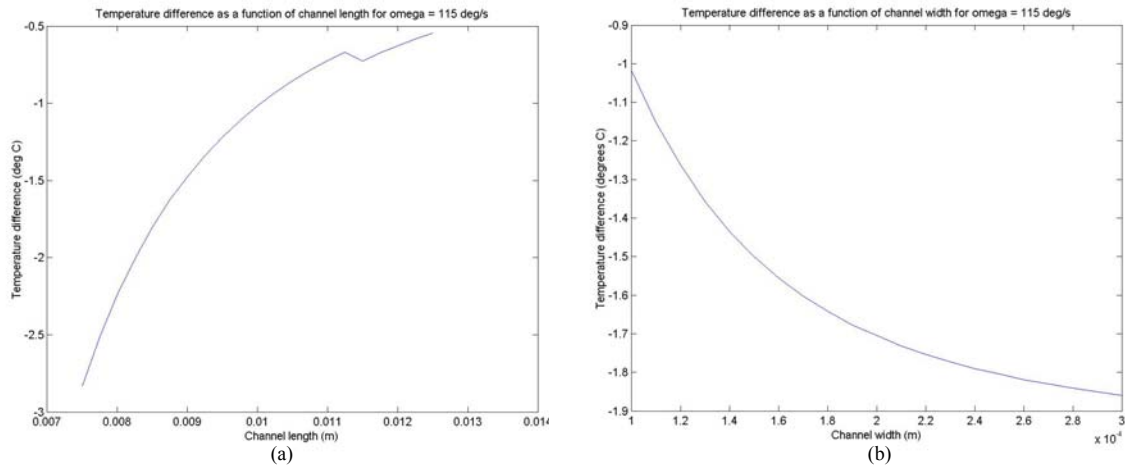
### Device Response: Rate Resolution, Linearity and Sensitivity

Figure 6 shows that the device responds linearly to inputs of up to 150 deg/s in magnitude with a sensitivity of approximately 0.75 deg/s given the current state of the art in temperature sensing [11].



**Fig. 6:** Relation between yaw rate and differential temperature measurement

Figure 7 reveals the sensitivity of the device's performance to design changes. The geometry of the channel is shown to strongly affect the gyroscope response for given pressure drop and temperature gradient along the length of the channel. A non-linear dependence between the temperature



**Fig. 7:** Gyroscope sensitivity to channel geometry: length (a), and width (b)

difference and geometry results, indicating that decreasing the channel length and increasing its width positively affect the inertial sensor response. The gyroscope shows a linear dependence on the temperature and pressure gradient along the length of the channel. These parameters can be varied at the designer's discretion, thereby creating the possibility for substantial optimization of the device resolution, sensitivity and linearity.

### CONCLUSION AND DISCUSSION

In this paper, the principal of operation and design of a novel micromachined thermal gyroscope is studied. Numerical analysis shows that the device can operate over a linear range of  $\pm 150$  deg/s with a rate resolution of approximately 0.75 deg/s when appropriate nominal values for pressure and temperature drop across the channel are used. This inertial sensor could be used in "rate-grade" devices for automotive applications, although slightly more stringent requirements need to be satisfied on the yaw-rate resolution [12].

Experimental testing will be necessary in order to characterize the bandwidth and shock resistance of this new class of thermal gyroscopes. The test results reported for thermal accelerometers [6] relate the frequency response of the sensor to the thermal diffusivity and density of the gas. This suggests that the operating bandwidth of the device will be insufficient for many practical applications. Fluids other than water should be considered in order to improve the frequency response of the gyroscope. The absence of a vibrating proof mass should increase the shock resistance of the thermal yaw rate sensor, and hence provide greater sensitivity as reported for thermal accelerometers.

### REFERENCES

- [1] F. Ayazi, K. Najafi, "A HARPSS Polysilicon Vibrating Ring Gyroscope", *JMEMS*, vol. 10, no. 2, pp. 169-179, June 2001
- [2] J. Bernstein, *et al.*, "A micromachined comb-drive tuning fork rate gyroscope", *MEMS' 93*, pp. 143-148, Feb. 1993.
- [3] K. Maenaka, T. Shiozawa, "A study of silicon angular rate sensors using anisotropic etching technology", *Sensors and Actuators A*, vol. 43, pp. 72-77, 1994
- [4] R. Voss, *et al.*, "Silicon angular rate sensor for automotive applications with piezoelectric drive and piezoresistive read-out", *Transducers' 97*, pp. 847-850, June 1997
- [5] M. Hashimoto, *et al.*, "Silicon resonant angular rate sensor electromagnetic excitation and capacitive detection", *J. Micromech. Microeng.*, pp. 219-225, 1995
- [6] A. M. Leung, *et al.*, "Micromachined accelerometer based on convection heat transfer", *MEMS' 98*, pp. 627-630, January 1998
- [7] Y. Zhang, *et al.*, "A Micromachined Coriolis-force-based for direct flow and fluid density measurement", *Transducers' 01*, June 2001
- [8] X.B. Luo, *et al.*, "Thermal optimization on micromachined convective accelerometer", *Heat and Mass Transfer*, vol. 38, pp. 705-712, 2002
- [9] R.L. Panton, *Incompressible Flow*, New York: Wiley-Interscience, 1996
- [10] W.M. Kays, M.E. Crawford, *Convective Heat and Mass Transfer*, New York: McGraw-Hill, 1993
- [11] G. Kovacs, *Micromachined Transducers Sourcebook*, New York: McGraw-Hill, 1998
- [12] N. Yazdi, *et al.*, "Micromachined Inertial Sensors", *Proc. of the IEEE*, vol. 86, n.8, August 1998